A circumstellar disc in a high-mass star forming region

Michele R. Pestalozzi[1], Moshe Elitzur[2], John E. Conway[1] and Roy S. Booth[1]

michele@oso.chalmers.se, moshe@uky.edu, jconway@oso.chalmers.se,
roy@oso.chalmers.se

ABSTRACT

We present an edge-on Keplerian disc model to explain the main component of the 12.2 and 6.7 GHz methanol maser emission detected toward NGC7538-IRS1 N . The brightness distribution and spectrum of the line of bright masers are successfully modeled with high amplification of background radio continuum emission along velocity coherent paths through a maser disc. The bend seen in the position-velocity diagram is a characteristic signature of differentially rotating discs. For a central mass of $30 M_\odot$, suggested by other observations, our model fixes the masing disc to have inner and outer radii of $\sim 350\,\mathrm{AU}$ and $\sim 1000\,\mathrm{AU}$.

Subject headings: star formation – masers – Interstellar medium – discs

1. Introduction

Disks are expected to form during protostellar collapse, and low-mass stars seem to provide good observational evidence for the existence of disks (e.g. Qi et al. 2003; Fuente et al. 2003). The situation is less clear for high-mass stars. While in several cases velocity gradients in massive star forming regions have been detected on large scales ($> 10,000\mathrm{AU}$, e.g. Sandel et al. 2003), evidence for compact discs on scales $\lesssim 1000\,\mathrm{AU}$ remains sparse. One possible example is IRAS20126+4104, where there is good evidence for disc-outflow geometry around a $24 M_\odot$ central object (Cesaroni et al. 1999; Molinari et al. 2000). The case for a disc around G 192.16-3.82, a protostar of $\sim 15 M_\odot$ (Shepherd et al. 2001), is less compelling.

Class II methanol maser emission, a signpost of high mass star formation (Minier et al. 2001), offers a potential indicator of discs since it often shows linear structures in both space

---

[1]Onsala Space Observatory, SE-43992 Onsala, Sweden

[2]Department of Physics and Astronomy, University of Kentucky, Lexington, KY 40506–0055, USA

and position — line-of-sight velocity diagrams (Norris et al. 1998; Minier et al. 2000). These masers have been modeled as occurring at fixed radii within edge-on discs, although it is still unclear whether they arise primarily in discs or outflows (DeBuizer 2003; Moscadelli et al. 2002). One of the most striking examples of a maser line in both space and velocity is found in NGC7538-IRS1 N (Minier et al. 1998, 2000). We present here the first quantitative Keplerian disc analysis of this maser without invoking the assumption of a single radius. We find compelling evidence for the disc interpretation in this case.
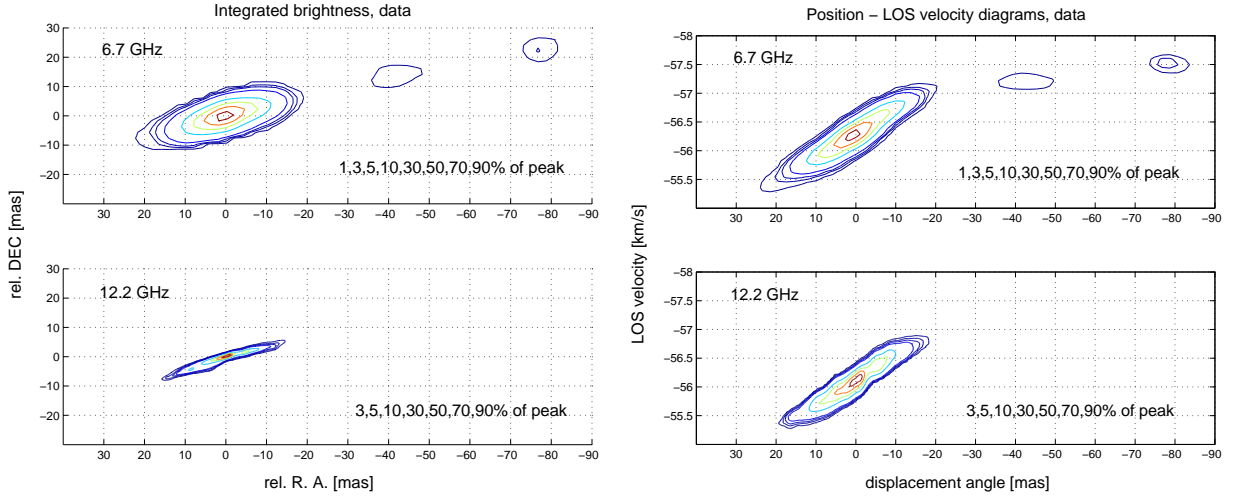

Fig. 1.— Left: Zero moment (integrated emission over velocity) maps of the 6.7 and 12.2 GHz methanol masers in the main spectral feature of NGC7538-IRS1 N . Right: (θ, v)-diagrams of the two masers, in which the data have been averaged over the spatial direction perpendicular to the major axis position angle.

2.   Maser data and other observations

The NGC7538-IRS1 star formation region has been extensively studied at several wavelengths. The spectral type of the central star has been estimated as O6 (Willner 1976; Campbell & Thompson 1984), in agreement with the SED from 2 mm (Akabane et al. 2001) to 850 μm (Momose et al. 2001) which implies a central object with luminosity of $> 8.3 \times 10^4 L_\odot$ and mass of about 30M$_\odot$. VLA observations uncovered an associated ultra-compact HII region with peak brightness temperature 10,000–15,000 K (Campbell 1984; Gaume et al. 1995). Radio free-free continuum and recombination line observations show a N-S elongated structure attributed to a large scale outflow.

The first VLBI observations of the 12.2 GHz methanol masers (Minier et al. 1998, 2000) revealed several groups of spots corresponding to different features in the single dish spectra. The subject of our study is the maser in the main spectral feature between about -56.50 and -56.82 km s^{-1}. The 12.2 GHz data cube from published data by Minier et al. (2001), made from 1998 VLBA[1] observations, is shown in Figure 1. The interpretation of the linear structure in space and velocity as an edge-on disc (Minier et al. 1998) is supported by the positional agreement of the maser line with the waist of the hour-glass shaped continuum radio emission (Gaume et al. 1995) and a band of free-free absorption. The same structure is evident in the 6.7 GHz maser data, obtained in February 2001 with the European VLBI Network (EVN[2]), shown in the figure. Taking into account the different angular resolution, the velocity-integrated emission of the two masers is similar out to ± 20 mas in R.A. (Figure 1, left). In addition, the 6.7 GHz data shows two disconnected 'outlier' maser features which lie close to the extrapolation of the maser line. The right panels in Figure 1 show the position-velocity diagrams for the two masers. They both show the same velocity gradient near the center and a bend at ~ 15 mas.

The 12.2 GHz line involves the $2_0 \rightarrow 3_{-1}E$ transition, the 6.7 GHz line the $5_1 \rightarrow 6_0 A^+$ transition. Since E- and A-methanol can be regarded as distinct molecules for all practical purposes, the two masers can be expected to probe different physical conditions even when they reside in the same region. Yet in spite of these differences, the brightness peaks of the two lines are perfectly coincident in both velocity and spatial location. The agreement is within the 12.2 GHz angular resolution of 2–3 mas and the spectral resolutions of 0.048 and 0.09 km s^{-1} per channel for the 12.2- and 6.7 GHz data, respectively. Convolving the 12.2 GHz data to the 6.7 GHz spatial resolution we find that the ratio of the two emissions is constant to within 10% over the entire feature.

3. Modeling

The remarkable coincidence in space and frequency of the two masers is in fact a natural consequence of amplification of a background source by an edge-on rotating disk. In that case the maser brightness at displacements θ and v from the position and velocity of the line-of-sight (LOS) diameter is $I(\theta, v) = I_{\mathrm{B}} \, e^{\tau(\theta, v)}$, where I_{B} is the background continuum and $\tau(\theta, v)$ the maser (negative) optical depth. Irrespective of the disk annuli where the masers

---

[1] The VLBA is operated from the National Radio AStronomy Observatory's Array Operation Center in Socorro, NM.

[2] The EVN is a joint facility of European, Chinese, South African and other radio astronomy institutes.

reside, the peak emission will always occur at $(\theta, v) = (0,0)$, which picks out the largest optical depth τ_0. With brightness temperature of 10^4 K for the background continuum, the function $\tau(\theta, v) = \ln\left[I(\theta, v)/I_{\rm B}\right]$ is a measured quantity. We find $\tau_0 = 18.32$ and 15.99 for the 6.7- and 12.2 GHz masers, respectively.

Consider an edge-on rotating disc at distance D and a point at radius $\rho = r/D$ along a path with displacement θ. The rotation velocity $V(\rho)$ and its LOS component v obey $v/\theta = V/\rho = \Omega$, the angular velocity. In Keplerian rotation $\Omega \propto \rho^{-3/2}$ with $\Omega_{\rm o} = \Omega(\rho_{\rm o}) = D\sqrt{GM/R_{\rm o}^3}$ where $\rho_{\rm o} = R_{\rm o}/D$ is the outer radius and M the central mass. Assume a Gaussian frequency profile for the maser absorption coefficient and denote the radial variation of its magnitude at line center by the normalized profile $\eta(\rho)$ ($\int \eta\, d\rho = 1$). Then

$$\tau(\theta, v) = \tau_0 \int \eta(\rho) \exp\left[-\tfrac{1}{2}\left(\frac{v - \Omega(\rho)\,\theta}{\Delta v_{\rm D}}\right)^2\right] \frac{d\rho}{\beta} \tag{1}$$

where $\beta = \sqrt{1 - (\theta/\rho)^2}$ and $d\rho/\beta$ is distance along the path. The width $\Delta v_{\rm D}$ is taken as constant, although it could vary with ρ because of temperature variation and maser saturation. Saturation typically requires $\tau \gtrsim 10$–15 across the disc radius, and the broadening of the absorption profile is then proportional to length in excess of this threshold (Elitzur 1992). If the NGC7538-IRS1 N disc is located in front of the background source then the overall amplification with $\tau \sim 18$ implies an optical depth of only 9 across the radius, too low for saturation. If the radio continuum is centered on the star then the optical depth across the radius is ~ 18 and saturation can be expected to have an effect, but only at the very outer segments of the disc where a decrease in temperature could have an opposite, offsetting effect. We will consider these effects in a future publication.

We parameterize η with a power law ρ^{-p} from an inner radius $\rho_{\rm i} = R_{\rm i}/D$ to $\rho_{\rm o}$. Both τ_0 and $\Delta v_{\rm D}$ are set directly from $\tau(0, v)$. Modeling the full $\tau(\theta, v)$ requires two free parameters for the integrand ($\Omega_{\rm o}$ and p) and two for the integration limits ($\rho_{\rm o}$ and $h = \rho_{\rm i}/\rho_{\rm o}$). Figure 2 shows contour plots of $\tau(\theta, v)$ for a representative Keplerian disc around a $30\,{\rm M}_\odot$ protostar with the $\Delta v_{\rm D}$ determined from the 12.2 GHz data at $\theta = 0$. The system is viewed edge-on at the adopted distance to NGC7538.

The lowest contour (3%) outlines the angular velocity $\Omega = v/\theta$ on the disk boundaries. The shallow segments of this contour (lower branch for $\theta < 0$) trace out the disk outer radius. The steeper ones trace the inner radius when $|\theta| < \rho_{\rm i}$ and the mid-line when $|\theta| > \rho_{\rm i}$, where the Keplerian $v \propto |\theta|^{-1/2}$ is evident. Along any path at $|\theta| < \rho_{\rm i}$, the velocity varies from $v_{\min} = \Omega_{\rm o}|\theta|$ on $R_{\rm o}$ to $v_{\max} = \Omega_{\rm i}|\theta|$ on $R_{\rm i}$. As long as $v_{\max} - v_{\min} < \Delta v_{\rm D}$, the full path remains velocity coherent and the maximal τ is centered on the velocity determined from $\partial\tau(v, \theta)/\partial v = 0$. This yields $v = \bar{\Omega}\theta$ where $\bar{\Omega} = \int \Omega\eta\, d\rho$, an average dominated by the high
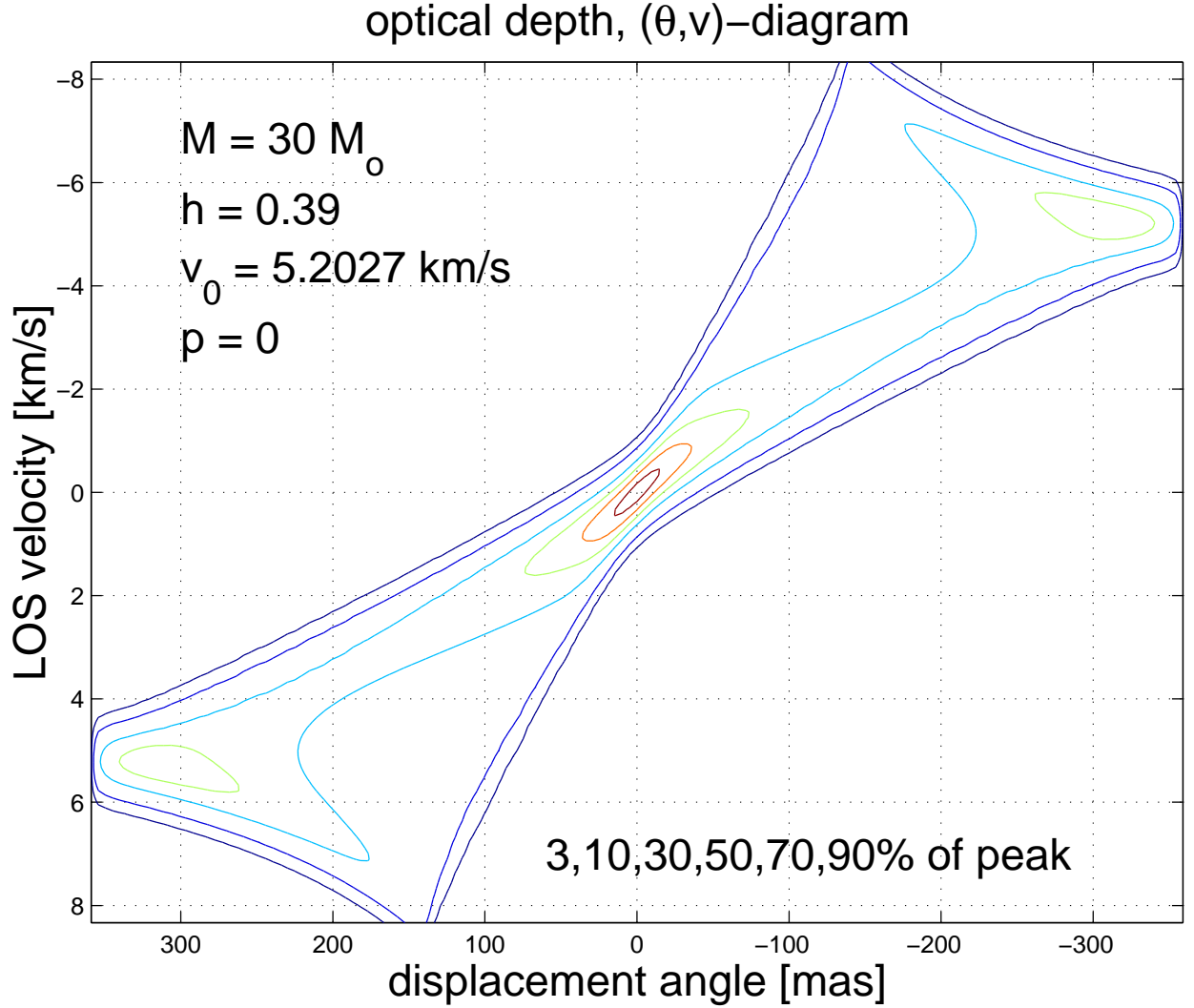
optical depth, (θ,v)−diagram

M = 30 M$_o$

h = 0.39

v$_0$ = 5.2027 km/s

p = 0

3,10,30,50,70,90% of peak

LOS velocity [km/s]

displacement angle [mas]

Fig. 2.— Contour plots of $\tau(\theta, v)$ (see eq. 1) for a Keplerian disc with Δv_{D} = 0.40 km s^{-1} around a $30\mathrm{M}_\odot$ star, viewed edge-on from $D = 2.7$ kpc. Constant maser absorption coefficient between radii $R_{\mathrm{i}} = 378$ AU (0''14) and $R_{\mathrm{o}} = 1080$ AU (0''4).

angular velocity of the inner regions; for example, constant η gives $\bar{\Omega} = 2\Omega_{\mathrm{i}}h/(1 + h^{1/2})$. The linear relation between v and θ is evident in the uniform inclination of the innermost contours.

The condition $v_{\max} - v_{\min} = \Delta v_{\mathrm{D}}$ is met at a displacement θ_{k}, and τ gets contributions from only a fraction of the path when $\theta > \theta_{\mathrm{k}}$. Since the longest coherence is at the outer radius, where Ω is smallest, the τ-contours bend toward lower velocities as is evident in

the figure around $\theta_k \approx 0\rlap{.}''02$. This bending reflects the change from inner-edge to outer-edge dominance of longest coherence. As θ increases further beyond ρ_i, the longest coherent segment moves from the outer radius to the disc mid-line. The maximal τ begins to increase, creating the local outer maximum evident in the 50% contours at $\theta \approx 0\rlap{.}''39$ before final truncation at $\theta = \rho_o$.

This discussion shows that the contours of highest amplification, down to 70% of τ_0, contain dependence on p, h and Ω but not on ρ_o. This has two important consequences: (1) Successful modeling of the strongest maser emission requires one less parameter. (2) Since Ω involves only the combination M/R^3, the central mass cannot be determined without observations of (exponentially weaker) radiation close to the phase-space boundary to determine ρ_o.

Brightness measurements with dynamic range f map the τ-distribution between τ_0 and $\tau_0 - \ln f$. With $\tau_0 = 15.99$ and $f \simeq 100$, the 12.2 GHz data traces the τ-contours in NGC 7538-IRS 1 N down to 70% of peak. Therefore the data shown in the lower left map of figure 3 cover only the two innermost contours in figure 2, and if our model is applicable it should require only the three parameters h, Ω and p. In fact, the first two can be determined quite accurately even without detailed modeling since the bend in the τ-contours occurs at $v_k \simeq \frac{1}{2} \Delta v_D \left(1 + h^{3/2}\right)/\left(1 - h^{3/2}\right)$ and $\theta_k \simeq \Omega_m v_k$, where $\Omega_m = \frac{1}{2}(\Omega_i + \Omega_o)$. We find directly that $h = 0.39$ and $\Omega_m = 0.037 \, \mathrm{km\, s^{-1}}$/mas, implying $M/R_o^3 = 30 \mathrm{M}_\odot/(1000\mathrm{AU})^3$ and leaving p as the only free parameter to match all other data points in the (θ, v)-plane. Sensible fits to the 12.2 GHz data are obtained when $0.035 \lesssim \Omega_m \lesssim 0.045$ and $0.3 \lesssim h \lesssim 0.4$.

The lower right panel of figure 3 shows the model map for $p = -0.5$, the top panels show how well the fitting of $\tau(\theta, v)$ reproduces the brightness profile and the spectrum. The negative p means that η, i.e., the maser absorption coefficient, increases with radius. The relation between η and overall density involves the product of the methanol abundance, the fraction of methanol in the maser system and the fractional inversion. Any of these factors might give more weight to the disk outer regions. Considering the simple power law with sharp cutoffs we employ, a 70% increase in η across the disk is compatible with a constant density profile.

Our model is equally successful in fitting the main 6.7 GHz maser emission, as is evident from figure 4. The value of p is the same for this maser, the only slightly different parameters are $\tau_0 = 18.32$, $h = 0.38$ and $\Omega_m = 0.037$ km/s/mas. The value for Δv_D was taken from the 12.2 GHz maser, which is considered to be more reliable because of the higher spatial resolution. Good fits of the 6.7 GHz data are obtained when $0.035 \lesssim \Omega_m \lesssim 0.045$ and $0.35 \lesssim h \lesssim 0.45$. The virtual identity of the disc segments of such different masing transitions is an important challenge for class II methanol pumping calculations.

4. Discussion

The analysis presented here shows that a Keplerian disk explains successfully, down to minute details, the main methanol maser feature in NGC7538-IRS1 N . The angular velocity we find implies a disk outer radius of $\sim$1000 AU if the central mass is $30M_\odot$, as determined by Campbell (1984). The methanol maser emission covers a substantial area of the disk, with the radius varying by a factor of 3.

The $\tau(\theta, v)$-contours display a bend in the position-velocity diagram. Since $v = \Omega\,\theta$, a straight line in this diagram implies a constant $\Omega(\rho)$, i.e., either a single radius or, in the case of an extended region, solid-body rotation. Our analysis therefore uncovers a unique signature of differential rotation in the NGC7538-IRS1 N disc. The emission's smooth structure and the observation's high sensitivity are crucial for this detection, which is made well inside the ~ 1.2 km s^{-1} width of the spectral feature (see top right panels in figures 3 and 4). These requirements preclude detection of the effect in extragalactic sources and explain why it could not be considered in the analysis of the H_2O maser disc in NGC4258 (e.g., Watson & Wallin 1994). However, a bend in the position-velocity diagram has been found in thermal line emission from low-mass stars and interpreted as steep-gradient solid-body rotation inside a shallow-gradient Keplerian outer region (Beckwith & Sargent 1993; Ohashi et al. 1997; Belloche et al. 2002). Since maser and optically thin thermal emission, which is directly proportional to optical depth, share the same kinematic structure, our analysis shows there is no need to invoke additional components on top of Keplerian rotation.

Our analysis is valid for a radio continuum source placed either behind the maser disc or at its center. The latter possibility would fit well in the context of disc photoevaporation models (Hollenbach et al. 1994). In that case, the radial extent of disc photoevaporation by the central star in NGC7538 covers the entire maser region and could activate both methanol formation and the observed outflow, responsible for the radio continuum. The maser location at the outflow waistline makes this scenario especially attractive.

The methanol maser data determines detailed disc properties with high precision yet the central mass remains undetermined since it requires the outer radius. And $\rho_{\rm o}$ is still unobservable because the angular extent of the detected emission does not trace the full disk, instead it is controlled by velocity coherence and the dynamic range of the observations. The amplification opacity at the disk outer edge (see fig. 2) is 50% of the central peak level. With $\tau = 16$ (18) at the center, detection of the outer peak requires a dynamic range of 3000 (8100) if the radio source is located behind the maser disc, placing it beyond the reach of the current observations by a factor of ~ 30 (80). The requirements become even more severe if the continuum is centered on the star. The 6.7 GHz outlier features therefore cannot correspond to the outer peak of our model disc. Instead, these outliers are probably the first

detection of enhanced amplification by small inhomogeneities in an otherwise rather smooth disc. Such non-axisymmetric distortions of the disk surface, and their possible effect on the pumping, have been proposed by Durisen et al. (2001). It should be possible, though, to determine ρ_o by probing the boundary of the (θ, v) region at $\theta < \rho_o$ along the v-axis or another direction such as the normal to $\bar{\Omega}$. We will study these issues in detail in a future publication.

This study provides one of the few pieces of evidence to date for a compact ($\lesssim 1000$ AU) disc around a massive protostar. It seems certain, though, that not all class II methanol masers occur in discs. Even in NGC7538-IRS1 N itself, the weaker methanol masers to the south, which are associated with other maser species (OH, H_2O etc), are likely to arise from an outflow. The interpretation of ordered lines of methanol masers in terms of disc or outflow models must be decided case by case with detailed modeling.

REFERENCES

Akabane, K., Matsuo, H., & Kuno, N. 2001, PASJ, 53, 821

Beckwith, S. & Sargent, A. 1993, ApJ, 402, 280

Belloche, A., André, P., Despois, D., & Blinder, S. 2002, A&A, 393, 927

Campbell, B. 1984, ApJ, 282, L27

Campbell, B. & Thompson, R. 1984, ApJ, 279, 650

Cesaroni, R., Felli, M., Jenness, T., et al. 1999, A&A, 345, 949

DeBuizer, J. 2003, MNRAS, 341, 277

Durisen, R.H., Mejia, A.C., Pickett, B.K., Hartquist, T.W., 2001, ApJL, 563, 157

Elitzur, M. 1992, ARA&A, 30, 75

Fuente, A., Rodriguez-Franco, A., Testi, L., et al. 2003, astro-ph

Gaume, R., Goss, W., Dickel, H., Wilson, T., & Johnston, K. 1995, ApJ, 438, 776

Hollenbach, D., Johnstone, D., Lizano, S., & Shu, F. 1994, ApJ, 428, 654

Minier, V., Booth, R., & Conway, J. 1998, A&A, 336, L5

—. 2000, A&A, 362, 1093

Minier, V., Conway, J., & Booth, R. 2001, A&A, 369, 278

Molinari, S., Brand, J., Cesaroni, R., & F., P. 2000, A&A, 355, 617

Momose, M., Tamura, M., Kameya, O., et al. 2001, ApJ, 555, 855

Moscadelli, L., Menten, K., Walmsley, C., & Reid, M. 2002, ApJ, 564, 813

Norris, R., Byleveld, S., & Diamond, P. e. 1998, ApJ, 508, 275

Ohashi, N., Hayashi, M., Ho, P., & Momose, M. 1997, ApJ, 475, 211

Qi, C., Kessler, J., Koerner, D., Sargent, A., & Blake, G. 2003, astro-ph

Sandel, G., Wright, M., & Forster, J. 2003, ApJ, 590, L45

Shepherd, D., Claussen, M., & Kurtz, S. 2001, Science, 292, 1513

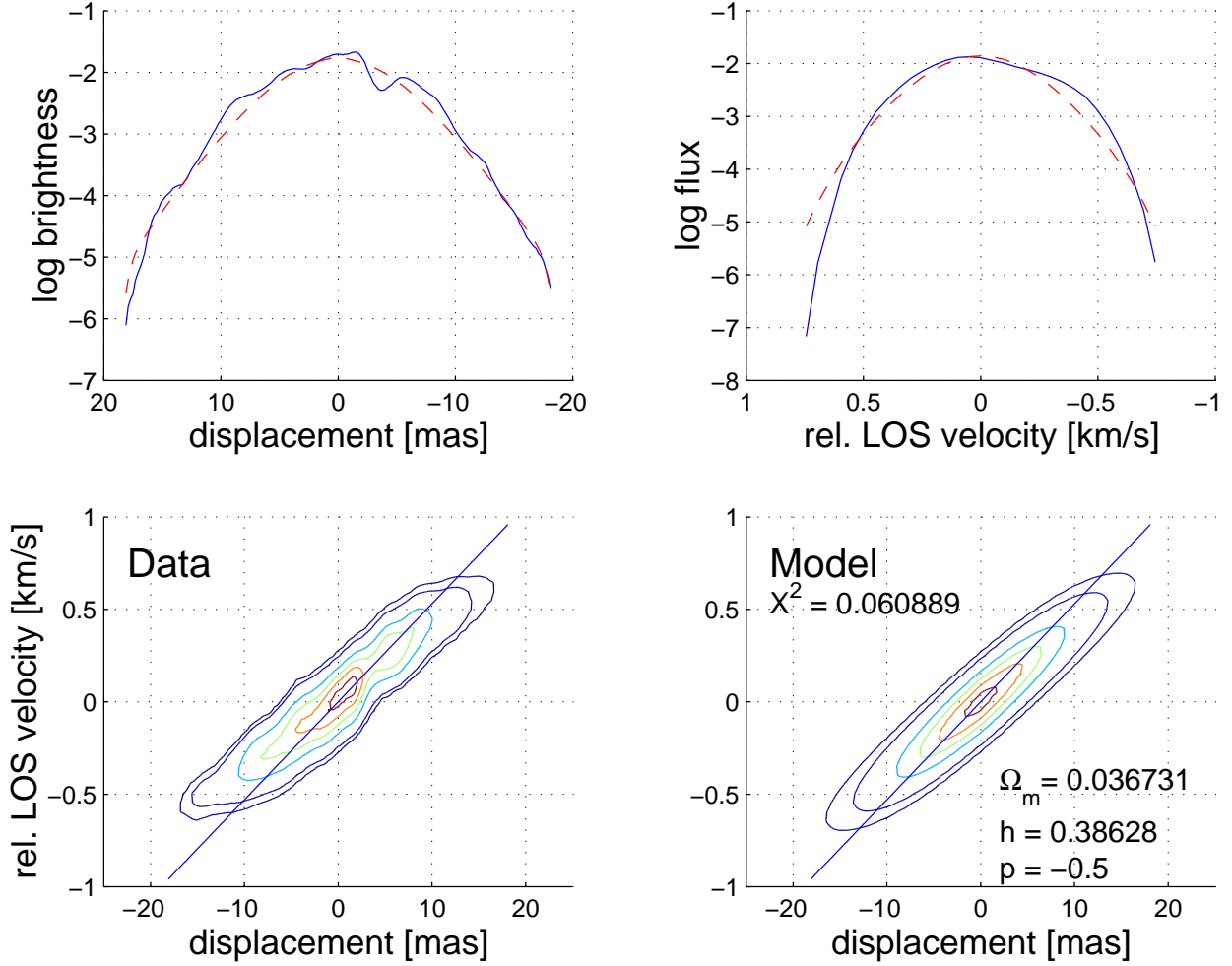Watson, W. & Wallin, B. 1994, ApJ, 432, L35

Willner, S. 1976, ApJ, 206, 728

Fig. 3.— Modeling the 12.2 GHz data with a disc with the indicated parameters and $\Delta v_{\mathrm{D}}=$ 0.4 km s^{-1}. Top: θ-variation of frequency-integrated brightness (left) and v-variation of the flux (right). In both diagrams the log of the quantities is shown. Solid lines show the data, dashed lines the model. Bottom: Contour plots of $I(\theta, v)$, the data to the left, the model to the right. The contours of the model have been obtained from the exponential of eq. 1. Contours are 5,10,30,50,70,90% of peak. The slope of the diagonal line is Ω_{i} in km s^{-1}/mas.
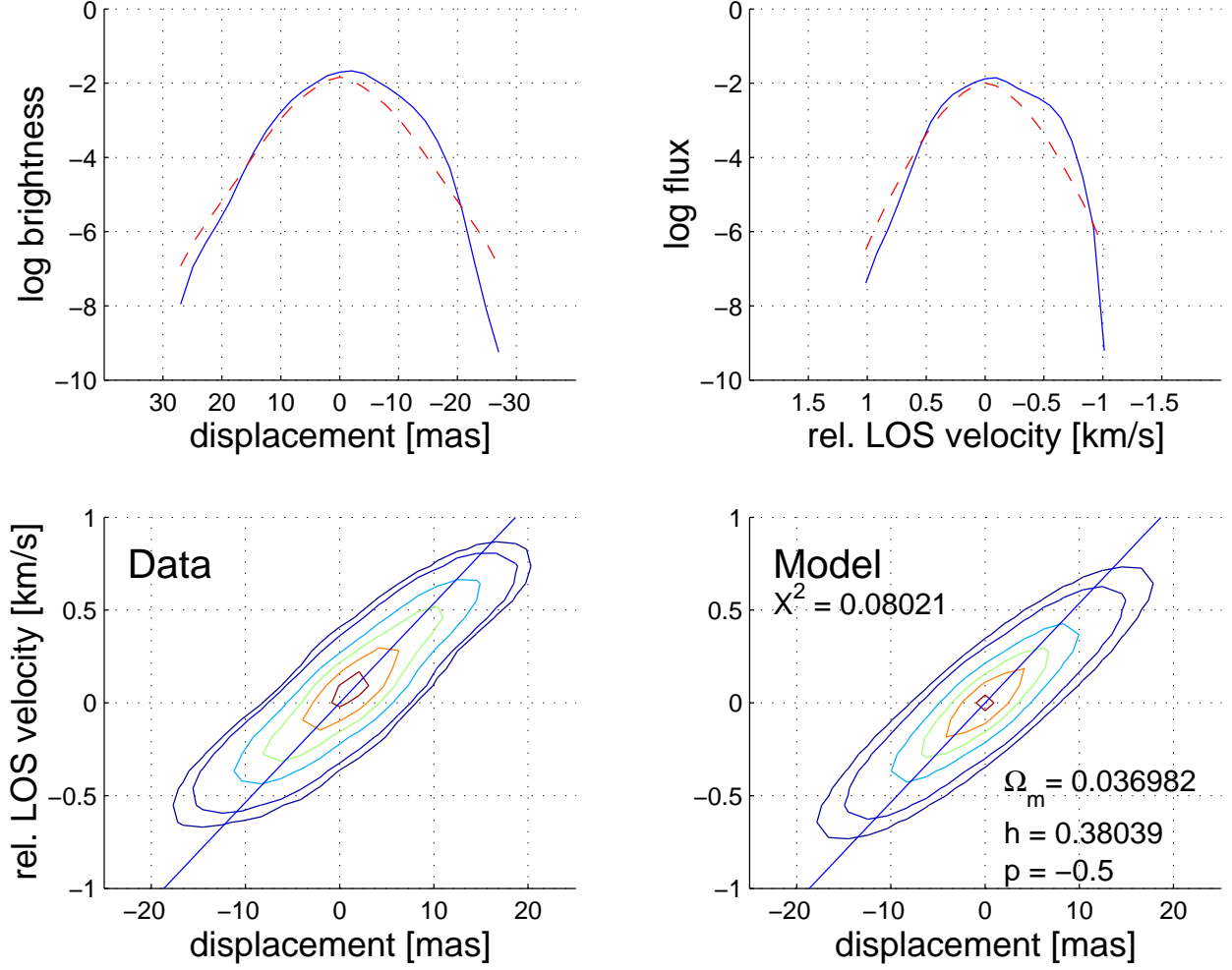
Fig. 4.— Same as figure 3 for the 6.7 GHz maser.